JCB Article

Abnormal neurofilament transport caused by targeted disruption of neuronal kinesin heavy chain KIF5A

Chun-Hong Xia,[1] Elizabeth A. Roberts,[1] Lu-Shiun Her,[1] Xinran Liu,[2] David S. Williams,[2] Don W. Cleveland,[3,4,5] and Lawrence S.B. Goldstein[1]

[1]Department of Cellular and Molecular Medicine, Howard Hughes Medical Institute, [2]Department of Pharmacology, [3]Ludwig Institute for Cancer Research, [4]Department of Medicine, and [5]Neuroscience, University of California, San Diego, La Jolla, CA 92093

To test the hypothesis that fast anterograde molecular motor proteins power the slow axonal transport of neurofilaments (NFs), we used homologous recombination to generate mice lacking the neuronal-specific conventional kinesin heavy chain, KIF5A. Because null KIF5A mutants die immediately after birth, a synapsin-promoted Cre-recombinase transgene was used to direct inactivation of KIF5A in neurons postnatally. Three fourths of such mutant mice exhibited seizures and death at around 3 wk of age; the remaining animals survived to 3 mo or longer. In young mutant animals, fast axonal transport appeared to be intact, but NF-H, as well as NF-M and NF-L, accumulated in the cell bodies of peripheral sensory neurons accompanied by a reduction in sensory axon caliber. Older animals also developed age-dependent sensory neuron degeneration, an accumulation of NF subunits in cell bodies and a reduction in axons, loss of large caliber axons, and hind limb paralysis. These data support the hypothesis that a conventional kinesin plays a role in the microtubule-dependent slow axonal transport of at least one cargo, the NF proteins.

Introduction

Axonal transport in neurons is essential because of the extreme polarity and size of these cells. In humans, some neurons, such as spinal motor and sensory neurons, extend axons of 1 m or more in length to reach postsynaptic targets in the periphery. Because the axon has little or no protein synthesis machinery, axonal proteins must be synthesized in the cell bodies and transported to the nerve terminals via axonal transport. Membranous organelles, such as synaptic vesicle precursors, mitochondria, and other vesicles, are transported by the fast axonal transport system. Cytoskeletal proteins, such as neurofilament (NF)* proteins, are moved by the slow axonal transport system.

Although numerous studies demonstrate that kinesin and its relatives are the motor proteins driving fast anterograde axonal transport, the existence and identity of motor proteins powering slow axonal transport have been controversial and mysterious. Some experiments suggest that NF subunits move anterogradely in axons through a microtubule- and energy-dependent mechanism (Koehnle and Brown, 1999; Yabe et al., 1999). Other in vitro experiments suggested the possible involvement of conventional kinesin (called kinesin-I) in the slow axonal transport of NF-L (61 kD), NF-M (90 kD), and NF-H (115 kD) (Yabe et al., 1999). Kinesin-I was also reported to associate with vimentin-containing structures in nonneural cells (Prahlad et al., 1998). Recently, GFP-tagged NF-M has been shown to move in a rapid, intermittent, and highly asynchronous manner in cultured nerve cells (Wang et al., 2000). Together these observations have raised the possibility, still not rigorously tested, that the slow rate of slow axonal transport may be the result of rapid movements driven by a fast motor protein interrupted by prolonged pauses. Thus, it is possible that a fast axonal transport motor such as kinesin-I could be involved in the transport of these intermediate filament proteins at a slow net rate.

Kinesin-I was first found in squid axoplasm and was the first identified member of the kinesin superfamily (Brady, 1985; Vale et al., 1985). Native kinesin-I is a heterotetramer composed of two kinesin heavy chain (KHC) subunits (110–130 kD) and two kinesin light chain (KLC) subunits (60–70 kD) (Bloom et al., 1988). KHC has a motor domain that interacts with the microtubule track and hydrolyzes ATP. KLC subunits are probably involved in cargo binding or mod-

Address correspondence to Dr. Lawrence S.B. Goldstein, HHMI/CMM-West Room 336, University of California, San Diego, 9500 Gilman Drive, La Jolla, CA 92093-0683. Tel.: (858) 534-9702. Fax: (858) 534-9701. E-mail: lgoldstein@ucsd.edu

*Abbreviations used in this paper: c-section, caesarian section; DRG, dorsal root ganglion; E, embryonic day; ES, embryonic stem; KHC, kinesin heavy chain; KLC, kinesin light chain; NF, neurofilament.

Key words: slow axonal transport; neuronal kinesin heavy chain KIF5A; neurofilament; axonal caliber; DRG sensory neuron

The Journal of Cell Biology, Volume 161, Number 1, April 14, 2003 55–66
http://www.jcb.org/cgi/doi/10.1083/jcb.200301026

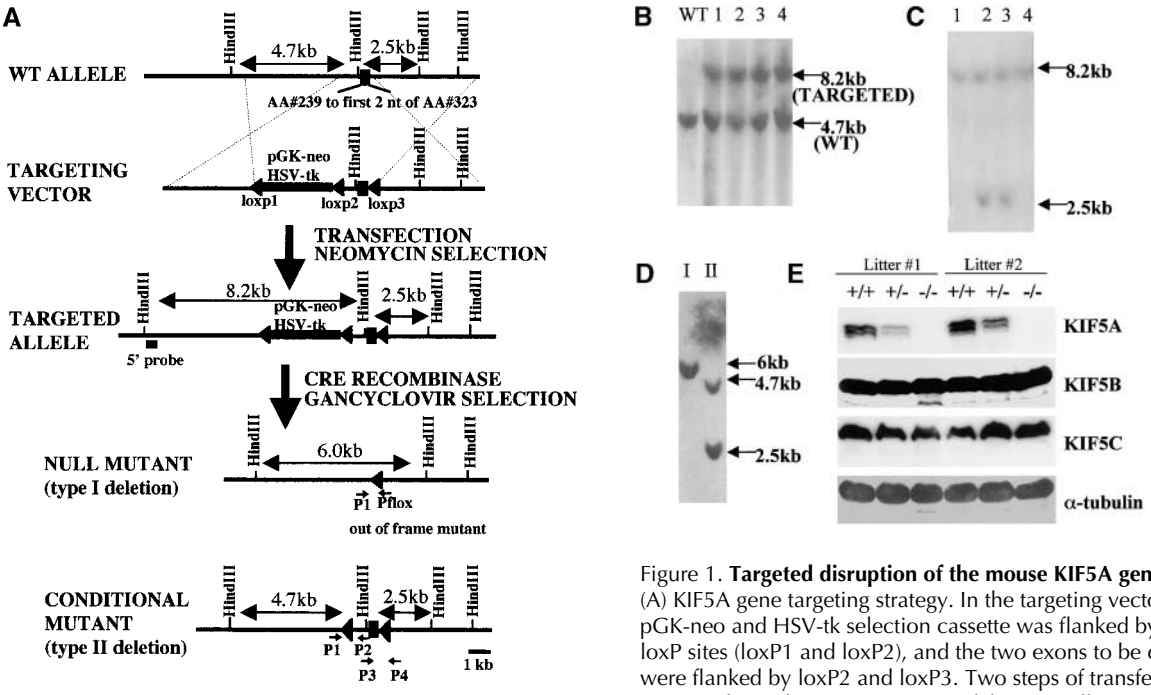

Figure 1. **Targeted disruption of the mouse KIF5A gene.** (A) KIF5A gene targeting strategy. In the targeting vector, the pGK-neo and HSV-tk selection cassette was flanked by two loxP sites (loxP1 and loxP2), and the two exons to be deleted were flanked by loxP2 and loxP3. Two steps of transfection were performed to generate type I deletion (null mutant) and type II deletion ES cells. The first step was done by transfecting linearized targeting vector into ES cells followed by G418 selection; the second step was performed by transfecting a Cre plasmid into recombinant ES cells isolated from the first step, followed by Gancyclovir selection. (B and C) Southern blot analyses of HindIII-digested G418-resistant ES clones after transfecting targeting vector. (B) A 5′ external probe was used to identify the recombinant clones. A 4.7-kb wild-type band was detected, and an additional 8.2 kb (with the addition of a 3.5-kb selection cassette) was also detected in the recombinant clones. (C) The presence of three loxP sites was confirmed by a loxP probe. The correct recombinant clones should have all three loxP sites, both 8.2-kb and 2.5-kb bands should be detected by the probe (clones 2 and 3), whereas clones 1 and 4 only had the first two loxP sites. (D) Southern blot analysis of HindIII-digested Gancyclovir-resistant clones after Cre transfection. With the loxP probe, only a 6-kb band was detected in type I deletion (KIF5A^{null}) ES cells, whereas 4.7-kb and 2.5-kb bands were detected in type II (KIF5A^{flox}) ES cells. (E) No KIF5A protein was detected in KIF5A null mutant mice by Western blot analysis. Mouse brain homogenates were made from two litters of mice, and 100 μg of protein was loaded in each lane. Isoform-specific antibodies were used to probe KIF5A, KIF5B, and KIF5C; α-tubulin was used as a loading control.

ulation of KHC activity (Bloom and Endow, 1995; Goldstein and Philp, 1999; Rahman et al., 1999; Kamal et al., 2000). Although only one conventional KHC gene is found in many species, including *Drosophila melanogaster* and *Caenorhabditis elegans*, mammals have three KHC genes (KIF5A, KIF5B, and KIF5C). KIF5B appears to be ubiquitously expressed, whereas both KIF5A and KIF5C appear to be expressed only in neuronal tissues (Navone et al., 1992; Niclas et al., 1994; Meng et al., 1997; Xia et al., 1998). The functions of KIF5A and KIF5C are unknown, although KIF5C has been suggested to be important for the viability of motor neurons (Kanai et al., 2000), and KIF5A mutations have been found to cause a form of hereditary spastic paraplegia in humans (SPG10; Reid et al., 2002). Although conventional kinesin has been suggested to play a role in the slow axonal transport of NFs (Koehnle and Brown, 1999; Yabe et al., 1999), the identity of the KHC isoform that might be involved is unclear. To investigate the function of KIF5A, and to test the role of KIF5A in the slow axonal transport of NFs, we have now generated and analyzed null and conditional KIF5A mutants in mice.

Results

KIF5A null mutants were lethal

We made a KIF5A deletion mutant by homologous recombination. The strategy (Fig. 1 A) was to create a null mutant by deleting two critical exons, causing a frame shift of the encoded protein. Mice heterozygous for the KIF5A null mutation were mated, and 33 newborn offspring from four litters were analyzed. Initial genotyping revealed that no KIF5A homozygous mutants survived, only three dead homozygous pups were found. Thus, KIF5A null mutants are probably neonatal lethal. To directly observe the behavior of KIF5A null mutants, KIF5A heterozygous mice were mated, the pregnant female mice were killed by caesarian section (c-section), and the embryonic day 18.5 (E18.5) pups were genotyped. Although live null mutant pups were never observed by natural birth, all null pups recovered by c-section were alive at E18.5. Whereas control littermates quickly developed a normal breathing pattern, the mutant pups did not (although like control littermates, they gasped just after removal from the uterus). Mutant pups gradually turned blue and usually died within 10 min. In a mixed 129/C57BL background, a total of 45 litters of E18.5 pups obtained by c-section were PCR genotyped. The predicted Mendelian ratio of 1:2:1 was observed: wild type (83/309), heterozygous (153/309), and homozygous mutant (73/309). The KIF5A homozygous mutant pups were indistinguishable from their control littermates by size and appearance. No visible structural defects were observed in any organs.

Immunoblots with a KIF5A polyclonal antibody of brain extracts of wild-type, heterozygous, and homozygous KIF5A

mutant littermates revealed that KIF5A was totally absent in the homozygous mice (Fig. 1 E). Heterozygous mice had reduced KIF5A as expected. Reprobing the blot with KIF5B and KIF5C antibodies showed no significant change in the amount of either in the KIF5A mutant.

Because KIF5A null mutant pups delivered by c-section died soon after birth and did not develop a normal breathing pattern as control littermates did, lungs from mutant and control littermates were sectioned and stained with hematoxylin-eosin. KIF5A mutant lungs did not expand as well as those of control littermates (Fig. 2 A). Thus, unexpanded lungs may be the cause of death, although the nature of the underlying mechanism is unclear. The diaphragm muscle was studied by immunostaining and electron microscopy to examine whether the neuromuscular junction region and muscle structure developed normally. No consistent abnormality was found in the mutant (unpublished data).

Because KIF5A is only found in neurons, histological analysis of the brain and spinal cord was performed. No obvious pathological changes were observed in the KIF5A mutant brain (Fig. 2, D–F). Interestingly, nuclei and cell bodies of spinal cord motor neurons of the KIF5A mutant appeared to be bigger than motor neurons of control littermates (Fig. 2, B and C). Hippocampal neurons cultured from KIF5A null mutants did not show any morphological difference when compared with cells from control littermates. Electrophysiology of these cells did not reveal any defect in synaptic transmission caused by the absence of KIF5A (unpublished data).

Cre-mediated postnatal loss of KIF5A causes seizures and sensory neuron degeneration

To understand better the lethality caused by loss of KIF5A, and to test whether KIF5A might have a role in slow axonal transport of NFs, we constructed a conditional KIF5A mutant, which was combined with a transgene encoding the Cre recombinase under the control of the synapsin I promoter ($Cre^{synapsin}$) (Zhu et al., 2001). This transgene is known to be a neuron-specific, developmentally regulated gene whose expression follows a biphasic postnatal time course with a maximum around day 20 (Hoesche et al., 1993). By mating $KIF5A^{flox}/KIF5A^{flox}$ mice to $KIF5A^{null}/KIF5A^{WT}$; $Cre^{synapsin}$ mice, $KIF5A^{null}/KIF5A^{flox}$; $Cre^{synapsin}$ offspring were identified.

Quantitative immunoblot analysis of a small set of initial animals showed that KIF5A protein levels in mutant brains ranged from 6 to 56% of that of control brains (Fig. 3 A). The heterogeneity in the level of reduction of KIF5A may reflect variable efficiency of Cre-mediated gene excision. To observe directly KIF5A excision at the cellular level, dorsal root ganglion (DRG) and spinal cord from ~3-wk-old mutants were examined by immunostaining with a KIF5A-specific antibody (Fig. 3, B and C). This staining

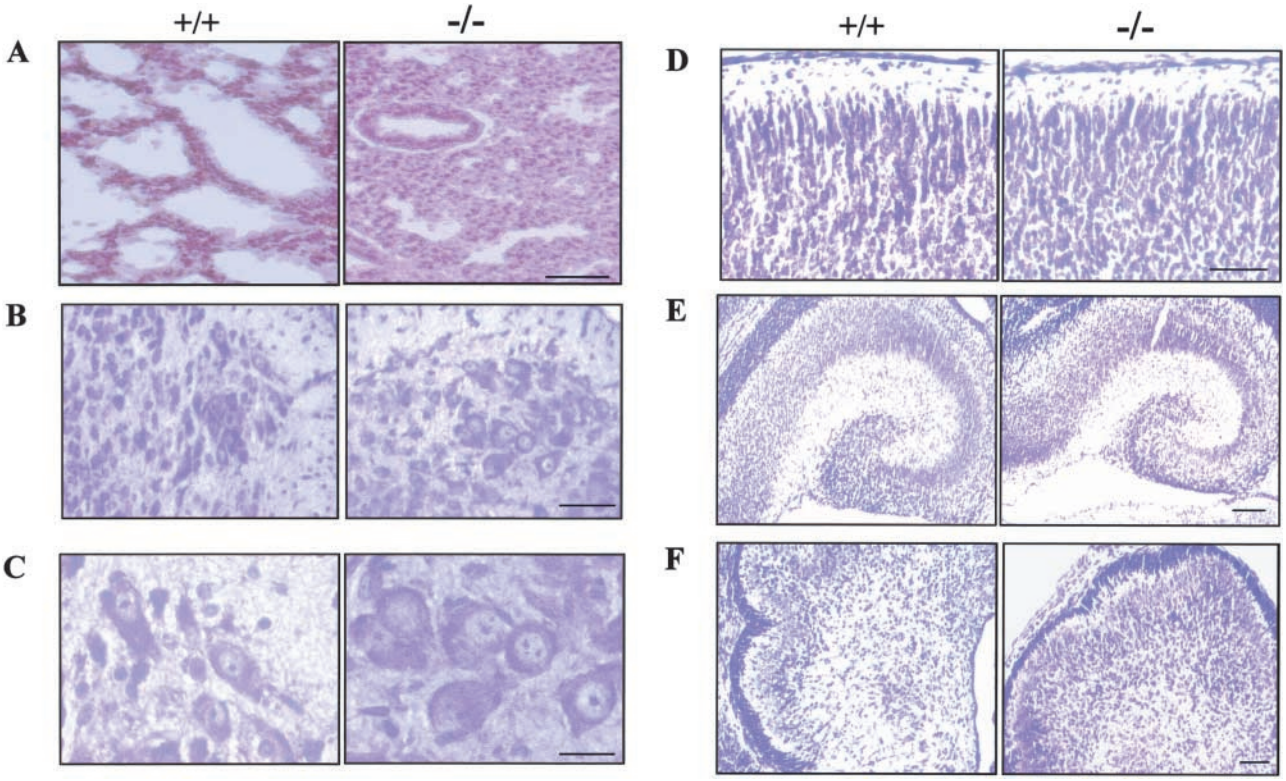

Figure 2. **Histology of KIF5A null mutant mice.** (A) Lung histology of KIF5A null mutant. 7-μm lung paraffin sections from KIF5A null ($KIF5A^{null}/KIF5A^{null}$) and control ($KIF5A^{WT}/KIF5A^{WT}$) littermates were stained with hematoxylin and eosin. Note that the mutant lung was not well expanded. Bar, 50 μm. (B–F) Histology of KIF5A null mutant nervous tissues. Paraffin sections from spinal cord (B and C), cortex (D), hippocampus (E), and cerebellum (F) were stained with cresyl violet. Note that no obvious differences were observed between KIF5A null mutant and control littermates except that the cell bodies of the motor neurons were larger in the mutant spinal cord. Bars: (B, D, and F) 50 μm; (C) 20 μm; (E) 100 μm.

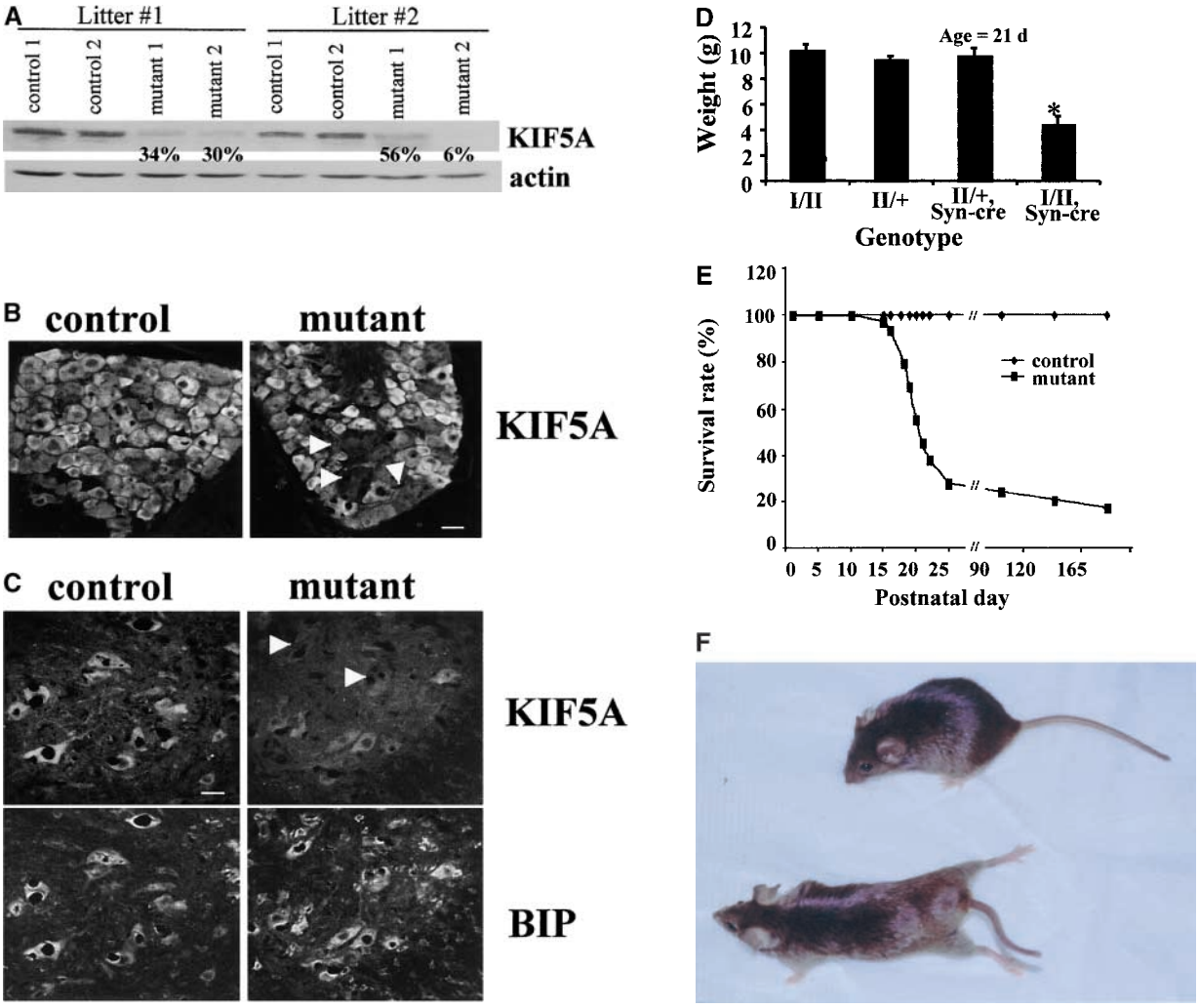

Figure 3. **Gross analysis of KIF5A conditional mutant mice (KIF5A^{null}/KIF5A^{flox}; Cre^{synapsin}).** (A) Western blot analysis to measure KIF5A protein levels in the brains of KIF5A^{null}/KIF5A^{flox}; Cre^{synapsin} mice. Equal amounts of brain homogenate from 3-wk-old mutant and control (KIF5A^{flox}/KIF5A^{WT}) littermates were loaded; actin was used as a loading control. Each marked number represents the ratio between the mutant band and control band after normalizing with the actin band. (B and C) KIF5A excision by Cre^{synapsin} transgene in DRG (B) and spinal cord motor neurons (C) of KIF5A^{null}/KIF5A^{flox}; Cre^{synapsin} mutant. Tissue sections from ~3-wk-old mutant and control littermates were stained with KIF5A-specific antibody. Spinal cord sections were also double stained with an anti-BIP antibody to visualize the motor neuron cell bodies. Note the decreased or lack of KIF5A staining in some neurons (arrowheads). Bar, 100 μm. (D) A comparison of body weight (mean ± SD) among 3-wk-old littermates with different genotypes. Note the obvious low body weight in the KIF5A^{null}/KIF5A^{flox}; Cre^{synapsin} mutant group, $n = 4$ for each group. *, $P < 0.01$. (E) Most KIF5A^{null}/KIF5A^{flox}; Cre^{synapsin} mutant mice died around 3 wk of age. Postnatal survival curve of a group of mice (142 total, 113 control and 29 mutant) is shown here. The rate of survival of the different genotypes was plotted against age. (F) Abnormal hind limb posture in an older KIF5A^{null}/KIF5A^{flox}; Cre^{synapsin} mutant mouse. Two 7.5-mo-old littermates (control and KIF5A^{null}/KIF5A^{flox}) are shown.

revealed an absence of KIF5A in some sensory neurons in the mutant. In spinal cord, costaining with a monoclonal BIP antibody (an endoplasmic reticulum marker) indicated that KIF5A staining in the mutant motor neuron cell bodies was much weaker compared with the control; some cells had almost no KIF5A staining. We conclude that KIF5A excision occurred in many DRG sensory neurons and spinal cord motor neurons.

As predicted, KIF5A^{null}/KIF5A^{flox}; Cre^{synapsin} mice survived the critical neonatal stage as did control littermates (KIF5A^{null}/KIF5A^{flox}, KIF5A^{flox}/KIF5A^{WT}, and KIF5A^{flox}/KIF5A^{WT}; Cre^{synapsin}). By 2–3 wk of age, however, mutant mice were obviously smaller than their littermates. At 3 wk, the weight of mutant mice was only ~50% of the control weight (Fig. 3 D). These mice responded to pinch (a crude sensory test), but they fell much more frequently than wild-type mice on a rotorod device (unpublished data). It is difficult to assess whether these problems result from motor defects or sensory defects. At 3 wk of age, KIF5A^{null}/KIF5A^{flox}; Cre^{synapsin} mutant mice exhibited a relatively normal posture, although they frequently exhibited a tremor.

In an initial cohort, 142 mice from 16 litters were followed (29 KIF5A^{null}/KIF5A^{flox}; Cre^{synapsin} mutant mice and 113 littermate control mice in a mixed 129/C57BL background), and survival curves were plotted (Fig. 3 E). 21/29 (72%) of the mutant mice died between day 15 and day 25; these mice appeared to die of seizures. Spontaneous seizures were observed as well as seizures apparently induced when

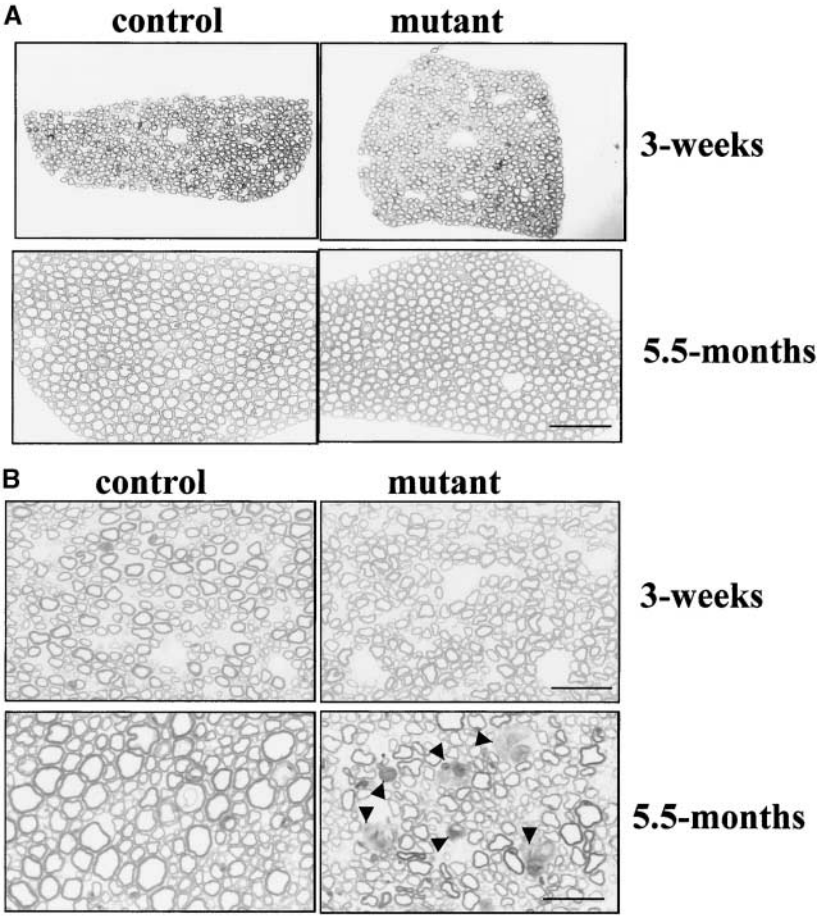

Figure 4. **Sensory axon degeneration in KIF5A^{null}/KIF5A^{flox}; Cre^{synapsin} mutant mice.** (A) Ventral roots of 3-wk-old and 5.5-mo-old mutant mice. Note the lack of degeneration. Bar, 50 μm. (B) Dorsal roots of 3-wk-old and 5.5-mo-old mutant mice. Note the lack of degeneration in 3-wk sensory axons, but in the 5.5-mo-old mutant, there are large numbers of degenerating axons (arrowheads) and a striking decrease of large caliber axons. Bar, 20 μm.

animals were stressed. Each seizure episode lasted ~20–30 s; repetitive seizure was observed, and the mice usually did not recover from severe seizures. Distinct from the 72% of mice that died at 3 wk of age, the remaining ~28% of mice lived >3 mo. This pool contains eight animals; among these eight mice, one died at 3 mo, one at 4 mo, and another at 5.5 mo (the remaining mice were killed for experiments at 5.5, 7, and 8 mo). All mutant mice that survived to 5 mo of age showed almost normal posture until ~5 mo (Fig. 3 F), but after that they developed a tremor when walking. The hind limbs behaved abnormally during walking, although they were not completely paralyzed, and the animals adopted abnormal hind limb posture during resting.

In spite of the obvious neuromuscular phenotype, no obvious morphological abnormality in spinal cord or DRG was observed in KIF5A^{null}/KIF5A^{flox}; Cre^{synapsin} mutants at either 3 wk or 7.5 mo of age (unpublished data). Examination of thin sections of ventral roots (Fig. 4 A) did not detect any obvious abnormality in 3-wk-, 5.5-mo-, or 7.5-mo-old mutant mice. Whereas no degeneration was detected in sensory axons of the dorsal roots from 3-wk-old animals (Fig. 4 B), four older mutant mice (two 5.5- and two 7.5-mo-old mice) showed striking degeneration of axons (Fig. 4 B), with numerous profiles of myelin debris (typical of Wallerian degeneration). This phenotype was not observed in the control littermates (KIF5A^{flox}/KIF5A^{WT} or KIF5A^{null}/KIF5A^{flox}). These data are consistent with an age-dependent onset of abnormal hind limb posture after loss of KIF5A.

Loss of large caliber axons and NF transport defects caused by postnatal loss of KIF5A

To determine quantitatively whether the loss of KIF5A affected the survival of motor and/or sensory axons, axons of the lumbar sciatic nerve roots were counted. Comparison of the number of L5 lumbar motor axons within ventral roots of 3-wk-old KIF5A-depleted mutants and control littermates (Fig. 5 A) revealed no significant axon loss ($P = 0.112$), indicating that loss of KIF5A had no significant effect on the survival of motor neurons at 3 wk of age. However, sensory axon numbers within dorsal roots (Fig. 5 A) were significantly reduced in the 3-wk-old KIF5A–synapsin Cre mutant animals (~86% of control; $P = 0.045$). Measurement of axonal diameter also revealed sensory loss reflected by a preferential loss of large caliber sensory axons. 60% ($P = 0.002$) of large caliber (>3 μm in diameter) sensory axons were lost, whereas no significant loss ($P = 0.26$) was observed for small caliber axons.

By 5.5 mo of age, we observed a small loss (~12%) of motor axons and a profound loss (~36%) of sensory axons (n = two control and two mutant animals) (Fig. 5 B). Again, sensory and motor (Fig. 5, C and D) axon loss was most substantial for axons >4 μm. Motor axons still showed a typical bimodal distribution of axonal sizes in both wild-type and KIF5A-depleted neurons, but the calibers of the large axons were clearly shifted to smaller sizes in the mutant group, and there was an obvious loss of >7.5-μm large caliber axons. In the dorsal roots (Fig. 5 D), profound

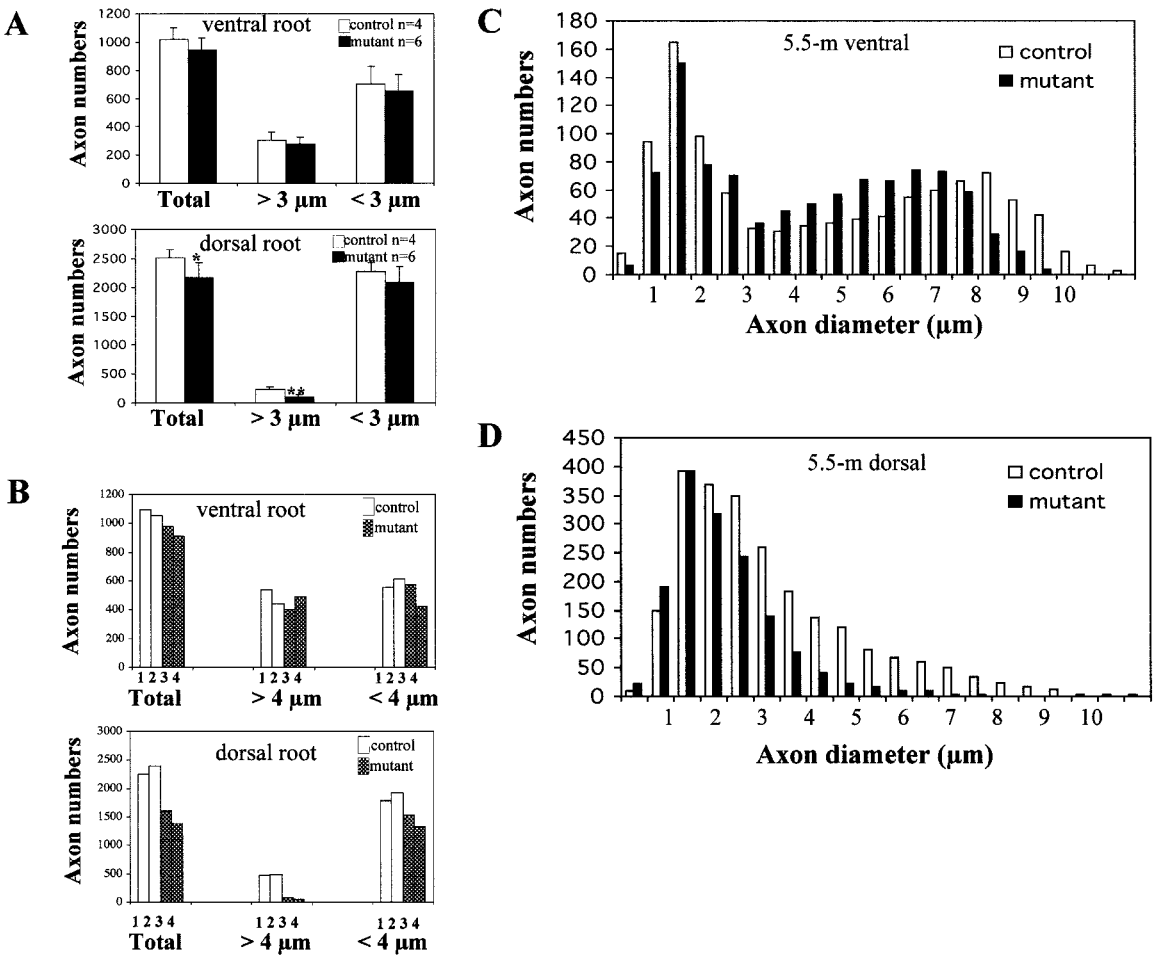

Figure 5. **Loss of large caliber axons in the KIF5A^{null}/KIF5A^{flox}; Cre^{synapsin} mutant mice.** (A) Counts of total, small (<3 μm diameter), and large (>3 μm diameter) myelinated axons in L5 ventral and dorsal roots from 3-wk-old control ($n = 4$) and mutant ($n = 6$) mice. No significant difference is observed between the number of mutant and control axons in the ventral root. There is a significant loss of dorsal root axons. *, $P < 0.05$ (0.045); **, $P < 0.01$ (0.002); *t* test. (B) Axon numbers of total, small (<4 μm), and large (>4 μm) myelinated axons in L5 ventral and dorsal roots from 5.5-mo-old control (1 and 2, control) and mutant (3 and 4, mutant) mice. There is a profound loss of dorsal root axons, especially large caliber axons. The loss of ventral root axons is not as profound as observed in the dorsal root. (C and D) Axonal diameters of L5 ventral root (C) and L5 dorsal root (D) from 5.5-mo-old mutant and control mice. Averaged distribution of axon diameters from the entire roots of two mutant and two control mice is shown. Note that in the ventral root (C), the peak of the distribution of the diameter of large caliber axons shifts from 7–7.5 μm in controls to 5.5–6 μm in mutants. Also note the obvious loss of large caliber axons in the dorsal root (D).

axon loss was observed in sensory axons with calibers >2 μm, with complete loss of the largest sensory axons (>7 μm), but no loss of small caliber sensory axons (<1.5 μm).

Many earlier efforts demonstrated that NF content in axons is a major determinant of axonal caliber (for reviews see Zhu et al., 1997, 1998). Concomitant with myelination beginning at weeks 2–3 and continuing through young adulthood (~5 mo), there is a rapid growth in axonal calibers (e.g., see Fig. 4, A and B). Loss of acquisition of the correct caliber by KIF5A-deficient axons, especially of the largest, most NF-rich axons, suggested that KIF5A might be one motor for NF transport into axons.

To test whether diminished axonal caliber was caused by reduced NF transport into, and accumulation within, sensory axons, we used immunoblotting of extracts of DRGs (comprised primarily of the cell bodies of sensory neurons). As expected if KIF5A was needed for efficient NF transport, NF subunits accumulated in KIF5A-depleted DRGs, while KIF5A levels were reduced to 20% of that in the controls (three litters were examined; one representative litter is shown in Fig. 6 A). A polyclonal antibody against the COOH terminus of NF-H, which recognizes NF-H independent of its phosphorylation state, revealed a significant (~150%) increase in total NF-H protein in mutant DRGs. The amount of NF-L was increased in mutant DRGs by an equivalent amount (~150%), while NF-M amounts were increased but to a lower extent (by 20–50%). The increase in NF-H was confirmed with the monoclonal antibody SMI-32, which is specific for the dephosphorylated isoform of NF-H, whereas a monoclonal antibody specific for phosphorylated NF-H (SMI-31) revealed a slight (10–15%) decrease. The type III intermediate filament protein peripherin was also increased in the mutant DRGs, whereas the neuron-specific βIII-tubulin isoform was not. Increases in NF-H, NF-M, NF-L, and peripherin were selective for the DRGs. No obvious changes in the amounts of NF-H,

NF-M, NF-L, or peripherin were found in the brain and sciatic nerve (Fig. 6 B).

We also examined NF levels in sensory neurons of four of the rare older surviving mice in which KIF5A was reduced by Cre-induced recombination (6 wk, 3 mo, 7 mo, and 8 mo). A variable phenotype was seen in these animals, possibly owing to variation in Cre-mediated KIF5A excision among these unusual surviving animals. Although the NF protein level was increased in the DRG of the 3-mo-old mutant animal, no obvious reduction in the amount of NF proteins was observed in the sciatic nerve. This animal, however, had very poor KIF5A excision. In the 7-mo-old mutant animal, obvious reductions in the content of NFs in the nerve and in the DRG were seen, perhaps because of sensory neuron degeneration. Significant reductions of NF-M, NF-L, and peripherin were observed in the sciatic nerves of the 6-wk-old and 8-mo-old mutants, accompanied by accumulations of these proteins in the DRGs. βIII-tubulin was modestly reduced in sciatic nerve samples of these animals, accompanied by a slight accumulation of these proteins in the DRGs. These changes appeared to be selective because the levels of other axonal proteins (KIF3A, KIF3B, and Rab5) were unaltered at both 3 and 6 wk of age in the mutant DRGs and sciatic nerves (unpublished data). Finally, the increased accumulation of NF-H observed by immunoblotting of the DRG was confirmed to reflect an increase in the amount within sensory neuron cell bodies, as judged by elevated staining in sections of DRG from mutants but not controls (Fig. 6, C and D).

To test further whether KIF5A mutants have a specific defect in slow axonal transport of NFs, we bred a second cohort of 12 3-wk-old KIF5A^{null}/KIF5A^{flox}; Cre^{synapsin} animals and 12 3-wk-old matched littermate control animals from five different litters. We used these animals to assess the integrity of several fast anterograde transport pathways (APP, Rab3, synaptophysin, and KIF5C), using a combi-

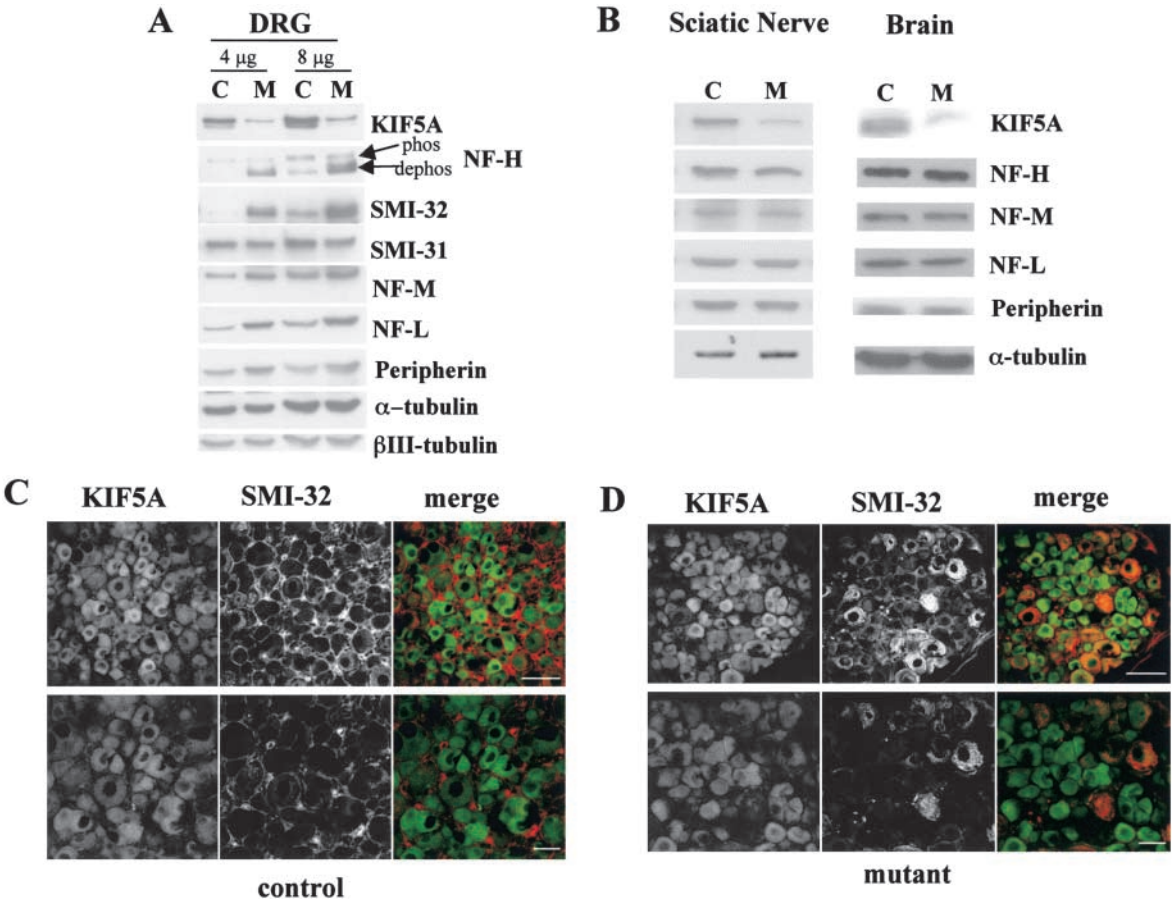

Figure 6. **Accumulation of NF proteins in DRG sensory neuron cell bodies of KIF5A^{null}/KIF5A^{flox}; Cre^{synapsin} mutant mice.** (A) Western blot analyses of DRGs from the first cohort of 3-wk-old KIF5A^{null}/KIF5A^{flox}; Cre^{synapsin} mutant mice. In the litter shown, control DRGs (C) were pooled from one II/+ and one Cre/+ littermates; mutant DRGs (M) were pooled from two mutant littermates. Note the obvious increase in dephosphorylated NF-H (revealed by the lower band labeled by NF-H, a polyclonal antibody against the COOH terminus of NF-H, and by antibody SMI-32) as well as the increase in NF-M, NF-L, and peripherin. (B) Western blot of brain and sciatic nerve from 3-wk-old KIF5A^{null}/KIF5A^{flox}; Cre^{synapsin} mutant mice. 20 μg of proteins of mutant and control (II/+) littermates was loaded in each lane. Note the clear reduction of KIF5A protein in the mutant. The levels of NFs and peripherin were not significantly changed in the mutant brain and sciatic nerve. (C and D) Immunostaining of DRG sensory neurons of 7.5-mo-old KIF5A^{null}/KIF5A^{flox}; Cre^{synapsin} mutant mice. Double staining with KIF5A (green) and SMI-32 (recognizes dephosphorylated NF-H, red) was performed on a mutant and a control littermate. (C) Control DRG staining. Bottom panel, higher magnification. (D) Mutant DRG staining, higher magnification in the lower panel. Note the apparent intense SMI-32 staining in some DRG neurons. Bars, 200 μm.

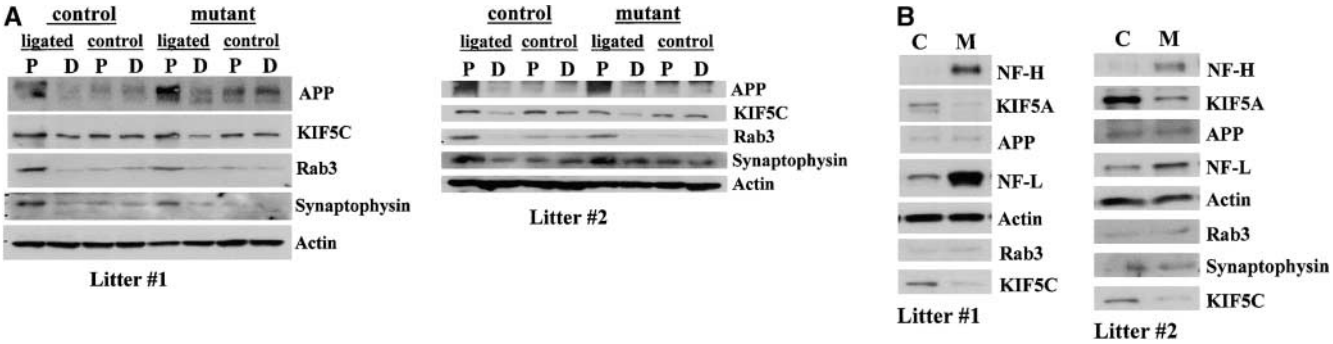

C SUMMARY OF SECOND COHORT OF 3 WEEK OLD KIF5A CONDITIONAL MUTANT MICE

PROTEIN LEVELS IN DRG (RELATIVE TO CONTROL)

	NF-H	NF-L	APP	RAB3	KIF5C	SYP	KIF5A
NORMAL	2/12	2/12	10/12	8/12	1/12	4/12	0/12
NOT DONE	0/12	0/12	2/12	4/12	3/12	8/12	2/12
ELEVATED	10/12	10/12	0/12	0/12	0/12	0/12	0/12
REDUCED	0/12	0/12	0/12	0/12	8/12	0/12	10/12

PROXIMAL ACCUMULATION AFTER LIGATION (RELATIVE TO CONTROL)

	APP	RAB3	SYP	KIF5C
NORMAL	10/12	9/12	9/12	9/12
NOT DONE	2/12	3/12	3/12	3/12
ELEVATED	0/12	0/12	0/12	0/12
REDUCED	0/12	0/12	0/12	0/12

Figure 7. **Analysis of DRG accumulation and axonal transport in second cohort of 3-wk-old KIF5A^{null}/KIF5A^{flox}; Cre^{synapsin} mutant mice.** (A) Axonal transport of APP, Rab3, synaptophysin, and KIF5C as assessed by Western blotting of proximal and distal segments 6 h after ligation of sciatic nerves from control and mutant animals; unligated controls are from the contralateral unligated nerve. Nerves from each animal were homogenized, and equal amounts of nerve proteins (~40 μg/lane) were loaded onto SDS-PAGE gels and analyzed by Western blotting. Data from two pairs of mice from different litters are shown. P, proximal side; D, distal side. (B) Analysis of DRG content of mutant and control animals. Approximately 12 μg of DRG lysate from each animal was loaded into each lane. Note increased NF-H and NF-L levels in the mutant DRGs, whereas protein amounts of APP, Rab3, and synaptophysin were not obviously changed. (C) Summary of data from 12 mutant and 12 littermate control animals from five litters. SYP, synaptophysin. As many antibodies as possible were used for reprobing of each filter, but filter lifetime was inconsistent so not all probes could be used on all animals.

nation of protein accumulation in sensory neuron cell bodies in DRGs and sciatic nerve ligation experiments (Kamal et al., 2000). Although the small size and fragility of the KIF5A animals and the technical difficulty in performing nerve ligations on them severely limited the sample amounts available, sufficient protein from sciatic nerve ligations of individual animals was obtained to load single lanes on gels and probe these multiple times with different antibodies (some of these filters could not be used for the full antibody set, yielding a reduced *n*; Fig. 7 C). As before, we observed significantly reduced KIF5A protein levels in all of the mutant DRGs compared with controls (Fig. 7), whereas the axonal transport profile of APP, Rab3, synaptophysin, and KIF5C was indistinguishable from that of their control littermates. 10 out of 12 KIF5A-deficient mice exhibited striking NF protein accumulation in the DRGs, whereas no significant changes in the protein levels of APP, Rab3, and synaptophysin were observed. Interestingly, KIF5C protein amount was slightly decreased in the mutant DRGs, although its abundance in the sciatic nerve and its transport behavior were comparable in the mutant and the control. Although further work will be necessary to understand the origin of KIF5C reductions in the DRG, one obvious possibility is that KIF5C may carry out functions that are redundant with those of KIF5A, such that when less KIF5A is available for transport, more KIF5C is used to compensate for the reduced function of KIF5A. Alternatively, KIF5C may form heterodimers with KIF5A (Kanai et al., 2000), and thus the amount of KIF5C may be decreased when its binding partner is reduced.

Discussion

Previous in vitro experiments raised the possibility that kinesin or kinesin family members are important for slow axonal transport of NFs in cell culture (Koehnle and Brown, 1999; Yabe et al., 1999) and squid axoplasm (Galbraith et al., 1999; Prahlad et al., 2000) models. This proposal has been highly controversial with unresolved issues including whether each of these systems even has the machinery for slow axonal transport.

We have shown here that although loss of KIF5A causes organismal lethality, mutant cells and tissues are remarkably normal in appearance, and most phenotypes assessed were normal. The only cellular phenotype we detected after postnatal removal of KIF5A was accumulation of NF subunits (NF-H, NF-L, and NF-M) and peripherin in the cell bodies of DRG sensory neurons. Evidence that this accumulation is a result of a specific deficit in slow axonal transport of NFs comes from our observation that markers of several fast axonal transport pathways (APP, Rab3, and synaptophysin) appeared unchanged in the DRG and in sciatic nerve ligation experiments. NF accumulation in the DRG was accompanied by a reduced number of the largest caliber sensory axons. βIII-tubulin was less consistent in its behavior because it was unchanged in younger animals, but showed behavior indicative of defective transport in some older animals; further work will be required to better understand whether KIF5A plays any role in βIII-tubulin transport. Although more complex interpretations are possible, the simplest conclusion from these findings is that KIF5A does not have a major role in typical kinesin-I fast axonal transport pathways, but does have a role in the in vivo transport of at least

one component of slow axonal transport, the NFs. The evidence also reveals an essential role for a conventional kinesin for normal postnatal radial growth; presumably a consequence of reduced slow transport of NFs, whose movement into axons is essential for such growth (Ohara et al., 1993; Eyer and Peterson, 1994; Zhu et al., 1997).

A fast motor in slow axonal transport?

Our quantitative immunoblot data showed a significant increase of NF-H, NF-M, and NF-L by 3 wk of age in the mutant DRGs, and thus in sensory neuron cell bodies. The simplest explanation is that these NF subunits were synthesized at normal rates but were moved out of the cell bodies at reduced rates. Overall, the levels of these proteins were not significantly changed in the brain, suggesting that the cell body accumulation is not caused by up-regulation of these proteins. Elevation of NF subunit levels in the DRG was not accompanied by obvious reductions in the sciatic nerve. This behavior is as expected based on two independent lines of evidence. First, the onset of the apparent deficit in transport is observed at 3 wk of age, the age at which substantial NF deposition and radial growth in axonal caliber normally begin. Only a subset of axons in mutants examined at this time have detectable caliber deficits (~250/3,500 total axons in the sciatic nerve). Second, although Cre-mediated excision using $Cre^{synapsin}$ has been detected as early as E12.5 (Zhu et al., 2001), it is likely that Cre excision is most active at 3 wk of age when synapsin-I promoter activity peaks (this would be consistent with the observation that ~72% of these mutants die at ~3 wk of age). Hence, animals at this age are most likely being analyzed not long after most recombination has occurred. We did observe reduced levels of NF-M, NF-L, and peripherin in the sciatic nerves of some older animals (unpublished data), consistent with the compromise in transport of NFs and peripherin in the KIF5A mutant. Our data are silent on the question of the form (subunit, oligomeric, or polymeric) of the transported material.

Our data are consistent with gene knockout studies of NFs that have provided evidence for their role in determining the calibers of large axons. NF-L gene knockout mice have no NFs and exhibit severe axonal hypotrophy (Zhu et al., 1997), and NF-M knockout mice showed profound reduction in NF number and reduction of axonal caliber in large myelinated axons (both motor and sensory axons) (Elder et al., 1998a; Jacomy et al., 1999). Three labs have reported on NF-H null mice. Two studies reported only a slight reduction in the caliber of myelinated axons from the ventral roots (Rao et al., 1998; Zhu et al., 1998), the third study described a more pronounced reduction in the caliber of motor axons (Elder et al., 1998b). One study also reported the consequence of loss of NF-H in sensory axons (Rao et al., 1998). Knockout of NF-H apparently inhibited the growth of the largest caliber sensory axons, ~19% of which were lost by 9 wk of age. Thus, NF-H plays an important role in the radial growth of sensory axons and, to a lesser extent, of motor axons.

One intriguing observation from our study is that DRG sensory neurons are more severely affected than motor neurons in the KIF5A–synapsin Cre mice. However, KIF5A is clearly present in both spinal cord motor neurons and DRG sensory neurons by immunolocalization. Two possible mechanisms could explain the phenotypic difference between motor neurons and sensory neurons. First, it is possible that KIF5A excision by Cre recombinase primarily or preferentially occurs in DRG sensory neurons but not in spinal cord motor neurons. Second, sensory neurons could have a specialized axonal architecture that is more dependent upon KIF5A for normal functions, including NF transport. Support for this latter possibility comes from our observation (unpublished data) that the levels of KIF5A are considerably higher relative to KIF5B and KIF5C in the DRG than in other neuronal tissues (brain, spinal cord, and sciatic nerve) examined. Evidence from other knockout mice also supports the notion that sensory neurons might have cytoskeletal and transport differences relative to motor neurons. For example, although both NF-L and NF-M knockout mice showed profound axonal atrophy (reduction of axonal caliber) in both motor neurons and sensory neurons, loss of NF-H in mice had very little effect on axonal calibers of motor neurons but apparently inhibited the growth of the largest caliber axons of sensory neurons (Rao et al., 1998). Similarly, deleting BPAG1n/dystonin, a protein that may form cross-bridges between NFs and actin filaments or NFs and microtubules, resulted in rapid degeneration of sensory neurons but not motor neurons, presumably due to perturbed axonal architecture (Guo et al., 1995; Yang et al., 1996, 1999). Another recent study suggested the possibility of a preferential requirement for another conventional kinesin, KIF5C, in maintenance of motor neurons (Kanai et al., 2000).

Although it is formally possible that loss of KIF5A has an indirect effect on transport of NFs in sensory neurons, a direct role of KIF5A in NF transport better fits our, and others', data (Yabe et al., 1999; Wang et al., 2000). In support of this view, our observation that fast axonal transport appears normal in KIF5A mutants suggests that changes in NF transport are not an indirect result of large defects in fast transport. How might a fast transport motor, kinesin-I, participate in slow axonal transport of NFs? A broadened peak of radiolabeled NF subunits during continued transport has been observed in various pulse-labeling experiments. It has been proposed that broadening of the transported wave of NFs reflects differential association and dissociation of individual NFs with their putative transport motor, i.e., the fastest moving NFs would represent those spending relatively more time in association with the motor, whereas the slowest moving NFs represent those that have dissociated from the motor for relatively longer periods (Lasek et al., 1992, 1993; Nixon, 1992, 1998a,b). Recently, axonal transport of an NF protein tagged with GFP has been directly observed in cultured nerve cells (Wang et al., 2000); the data led to the suggestion that the slow rate of slow axonal transport may be the result of rapid movements interrupted by prolonged pauses. Our data now provide a missing link, the identity of a motor that drives these movements. It is clear, however, that our data do not rule out the possibility that other motor proteins also participate in transport of NFs. Likely candidates include the other pair of conventional kinesins, KIF5B and KIF5C.

Are there other essential functions of KIF5A?

KIF5A was found to be essential for viability in neonatal animals. Because KIF5A is neuron specific, it is likely that this reflects a neuronal function that the other two KHCs (KIF5B and KIF5C) do not provide. Consistent with this view, the enlarged cell size of spinal cord motor neurons in the KIF5A null mutant suggests that the defects caused by loss of KIF5A could be related to nerve damage, perhaps reflecting impaired axonal transport of KIF5A cargoes. As all NF knockout mutants are viable, we presume that the transport of other, as yet unidentified, cargoes of KIF5A is essential, although it is possible that the neonatal death could be due to axonal blockage secondary to an NF transport defect. More studies need to be done to sort out these possibilities.

Recent work has revealed that KIF5A is defective in one form of hereditary spastic paraplegia (SPG10) (Reid et al., 2002), underscoring the importance of this protein and proper axonal transport for the health of the human nervous system. It is also striking that abnormal NF accumulations have been observed in many neurodegenerative diseases, including amyotrophic lateral sclerosis, Parkinson's disease, and Alzheimer's disease (Julien and Mushynski, 1998; Julien, 1999). It is possible that such accumulations are caused by impaired slow axonal transport of NFs, although the molecular basis of such blockage is obscure. KIF5A may turn out to be an important component of the machinery that fails in these disorders. Intriguingly, symmetrical sensory polyneuropathy, the most common form of diabetic neuropathy in humans, also has peripheral axonal degeneration, paranodal demyelination, and loss of myelinated axons (Zochodne, 1996; Yagihashi, 1997). Moreover, aberrant NF phosphorylation was observed in sensory neurons of rats with diabetic neuropathy (Fernyhough et al., 1999). In light of our finding that loss of KIF5A can provoke sensory axon degeneration, it will be of interest to test whether impaired axonal transport resulting from KHC impairment is involved in the development of these other diseases as well.

Materials and methods

Construction of the KIF5A targeting vector

A KIF5A genomic clone (encoding amino acids 98–547) isolated from a 129SVJ/Lambda FIX®II mouse genomic library (Stratagene) was used to construct the targeting vector. The KIF5A targeting vector was made as follows. An ~1.1-kb AvaII fragment containing two exons encoding amino acids 239–322 (VSKTGA to TLMFGQ) and the first two nucleotides for amino acid 323 was inserted into the BamHI site of the pflox vector by blunt ligation. An ~4.5-kb AvaII–SalI fragment (made by subcloning AvaII–EcoRV and EcoRV–SalI fragments, and then blunt ligated together in pSK) was blunt ligated into the XhoI site of the 1.1-kb AvaII/pflox, this 4.5-kb fragment was the right arm. The left arm was an ~3.2-kb XbaI–SpeI fragment, it was subcloned into the SalI site of the 1.1-kb AvaII + right arm/pflox by blunt ligation. For cloning convenience, an ~80-bp SpeI–AvaII intron sequence was deleted in the targeting vector, this probably would not affect the recombination efficiency and such a short intron sequence deletion also should not cause any phenotypic consequence. The finished targeting vector was designated as KIF5A-KO/pflox. The resulting vector had three loxP sites, the first two flanked the pGK-neo, HSV-tk selection cassette, the second and third loxP sites flanked the 1.1-kb AvaII fragment.

Generating chimeric mice and mouse tail DNA genotype

The KIF5A-targeted embryonic stem (ES) cells were generated as described by Wurst and Joyner (1993). The KIF5A-KO/pflox plasmid DNA was linearized with NotI and transfected into RI ES cells by electroporation. The ES cells were allowed to grow for 24–36 h before 200 μg/ml G418 (GIBCO BRL) was added for selection; ~120 neomycin-resistant ES clones were isolated after ~8 d selection. Four clones were homologous recombinant clones with three loxP sites; they were named as clones B2, B6, B18, and D17. Cre recombinase (PMC Cre pGK-Hyg) was transfected into D17 ES cells and 2 μM Gancyclovir was added to the medium 3–4 d after transfection, the surviving clones were picked up 5 d later. Among 48 clones selected, 30 clones were type I ES cells, 4 were type II ES cells. Type I ES clones D17-37 and D17-38 and type II clone D17-35 were injected into C57BL/6J blastocysts to produce chimeras. Male chimeras were used as founders to breed F1 hybrids with C57BL/6J female mice.

Mouse tail DNAs were made as described by Wurst and Joyner (1993) and were genotyped by PCR. Three primers (P1, P2, and Pflox) were combined to perform type I genotype, the 5′ primer P1 (GATACTCCAAGGCTGGGAACATA) and the 3′ loxP primer (Pflox kpnI, CGGTACCCGGGGATCAATTCGAG) will produce an ~300-bp mutant fragment, the P1 and P2 primers (TGTGGAGGTCAGAGGTCAAGT) will amplify an ~450-bp wild-type band. For type II genotype, a primer set P3 (CGTTCTGGACGAGGCAAAGA) and P4 (GATGGGACAGCAGCAGTGCA) will detect an ~370-bp wild-type band and an ~470-bp (with the addition of ~100 bp loxP sequence) type II band. A pair of specific primers (5′ primer, ACGTTCACCGGCATCAACGT; 3′ primer, CTGCATTACCGGTCGATGCA), which detects an ~300-bp band, was used for Cre transgene genotype. PCR conditions for all primer sets were denaturation at 95°C for 2 min, 30 cycles of denaturation at 95°C for 30 s, annealing and elongation at 72°C for 1.5 min, and a final elongation at 72°C.

Preparation of antibodies from KHC–His tag fusion proteins

DNA fragments encoding portions of the stalk region of KIF5A and KIF5C were subcloned into pET-23b (Novagen, Inc.) to generate COOH-terminal His-tagged fusion proteins. KIF5A fusion construct was made by subcloning a HincII–HindIII fragment (encoding amino acids 496–745, VNYDQKSQ to LQLELEKL) into pET-23b. KIF5C–His fusion protein construct was generated by subcloning a PCR fragment encoding amino acids 506–781 (DKTRANEQ to DKREQARE) into pET-23b. A comparable KIF5B fusion protein containing amino acids AVNYDQKS to QARQDLK was also generated in pET-23b.

Recombinant His-tagged KIF5A and KIF5C proteins were overexpressed by induction of transformed BL21 (DE3) bacteria at log phase with 0.5 mM IPTG for 2 h. The His-tagged fusion proteins were made as follows. The bacterial pellet was resuspended in lysis buffer ([solution A] 50 mM $NaPO_4$, 300 mM NaCl, 0.5 mM $MgCl_2$, 0.01% NP-40, and proteinase inhibitors) and lysed with a French press. The pellet, after a 25,000-rpm spin (15 min, Sorvall 647.5 rotor), was resuspended in 6 M urea (in solution A) for 1 h at 4°C, and then the Ni-NTA-agarose (QIAGEN) was added to the urea-solubilized fraction (by spin at 35,000 rpm in a Ti1270 rotor for 20 min) and incubated at 4°C for 60 min. The fusion protein–bound Ni-NTA-agarose was washed with 6 M urea/solution A, followed by a final wash with 20 mM imidazole/6 M urea/solution A, and the fusion proteins were eluted with 500 mM imidazole (in 6 M urea/solution A). SDS-PAGE gel slices of each fusion protein were injected into three rabbits to produce polyclonal sera against KIF5A or KIF5C.

Cross absorption and affinity purification were used to generate isoform-specific antisera. The affinity columns were prepared by coupling 20 mg of fusion proteins (reconstituted in 10 mM Hepes, pH 6.9, 50 mM NaCl, and 2 M urea with a Millipore Ultrafree®-4 centrifugal filter device Biomax-30 unit) to 2 ml of Affigel-15 (Bio-Rad Laboratories) for 1 h at RT. The uncoupled proteins were removed with several washes of 10 mM Hepes, pH 6.9, 50 mM NaCl, and the columns were blocked with 5% BSA for 1 h at RT, washed again, and lastly washed with 10 mM Tris (pH 7.5). The antisera were heated to 65°C for 15 min, diluted 10-fold in 10 mM Tris (pH 7.5), applied to the columns, and incubated overnight at 4°C. To generate KIF5A-specific antibodies, the rabbit antisera were applied to a KIF5B and KIF5C mixed fusion protein column, the flow-through (unbound supernatant) was applied to a KIF5A affinity column. The resins with bound KIF5A antibodies were washed with 10 mM Tris (pH 7.5), 0.5 M NaCl followed by three washes with 10 mM Tris. The antibodies were then eluted with 0.2 M glycine (pH 2.5) and neutralized with 1/10 volume of 1 M Tris (pH 8). The KIF5C-specific antibodies were generated by a similar strategy; passing through a mixed KIF5A and KIF5B column to immunodeplete cross-reacting antisera and binding to a KIF5C column to get KIF5C-specific antibodies.

Histology of mouse tissues

For KIF5A null mutants, dissected E18.5 mice brain and spinal cord were fixed in 4% paraformaldehyde/PBS overnight at 4°C. KIF5A–synapsin Cre

mutant mice were suffocated with carbon dioxide and transcardially perfused with 4% paraformaldehyde/PBS. Tissues were postfixed overnight at 4°C and then dehydrated and embedded in paraffin. Paraffin sections (7 μm) were stained with hematoxylin-eosin, or cresyl violet, and examined by light microscopy. Images were collected with a CCD camera.

For DRG root histology, animals were perfused with 4% paraformaldehyde/PBS, and half of the DRGs were removed and processed for immunostaining. The other half was fixed in 2% paraformaldehyde, 2.5% glutaraldehyde in PBS overnight at 4°C, postfixed in 1% osmium tetroxide in PBS for 1 h, washed, dehydrated, and embedded in Epon resin (Embed 812; Electron Microscopy Sciences). Semi-thin sections were stained with toluidine blue and examined by light microscopy.

Morphometric analysis

Axonal diameters were determined with a Bioquant Nova image analysis system (Bioquant R&M Biometrics, Inc.). In brief, 1-μm Epon sections of L5 lumbar roots were stained with toluidine blue and viewed under a 40× lens. All myelinated axons in each root were measured. The measured cross-sectional area of each axon was converted to a diameter of a circle of equivalent area.

Quantitative immunoblotting analysis

Mouse tissues were homogenized in RIPA buffer (50 mM Tris-HCl, pH 8.0, 150 mM NaCl, 1% NP-40, 0.5% sodium deoxycholate, 0.1% SDS). Homogenized tissues were quickly centrifuged (~1,000 *g* for 5 min in a microcentrifuge) to remove large debris. Protein concentrations were measured by Bradford assay (Bio-Rad Laboratories). Equal amounts of proteins from different genotypes were loaded on 7.5% SDS-PAGE, and the gels were transferred to PVDF membrane (Bio-Rad Laboratories). The protein blots were blocked in TBST (0.15 M NaCl, 10 mM Tris-HCl, pH 8.0, 0.1% Tween-20) with 5% milk and then probed with primary antibodies in the milk-TBST, followed by HRP-conjugated goat anti–rabbit IgG or anti–mouse IgG secondary antibodies (Jackson ImmunoResearch Laboratories). A chemiluminescence ECL kit (Amersham Biosciences) was used for developing the blots. The antibodies used for blotting were affinity-purified rabbit anti-KIF5A, used at 1:100 dilution; polyclonal Ab specific for KIF5C at 1:200; KIF5B-specific Ab (from R. Vale, University of California San Francisco, San Francisco, CA) at 1:100; monoclonal antibodies SMI-31 and SMI-32 (Sternberger Monoclonals Inc.) at 1:5,000; a polyclonal Ab against the COOH-terminal region of NF-H at 1:5,000; mouse anti–NF-M (clone RMO-44; Zymed Laboratories) at 1:1,000; mouse anti–NF-L at 1:5,000; rabbit anti-peripherin (Chemicon) at 1:1,000; rabbit anti-KIF3A at 1:1,000; rabbit anti-KIF3B at 1:1,000; rabbit anti–βIII-tubulin at 1:1,000; mouse anti-Rab3 (Synaptic Systems GmbH) at 1:1,000; rabbit anti-synaptophysin (Synaptic Systems GmbH) at 1:1,000; monoclonal anti-actin (Chemicon) at 1:5,000; and a monoclonal anti–α-tubulin Ab (clone DM1A; Sigma-Aldrich) at 1:10,000.

Immunostaining

Mice were euthanized with carbon dioxide and transcardially perfused with 4% paraformaldehyde/PBS. Tissues were removed by dissection and postfixed for 1–2 h at 4°C, followed by cryoprotection in 25% sucrose/PBS overnight. 10-μm cryostat sections were processed for immunofluorescence staining. Sections were blocked (5% BSA, 0.15% saponin in PBS) for 1 h at room temperature, followed by incubation in primary antibodies overnight at 4°C. The antibodies used for staining were rabbit anti-KIF5A at 1:20; monoclonal anti-Grp78 (BIP; StressGen Biotechnologies) at 1:200; and monoclonal Ab SMI-32 (Sternberger Monoclonals Inc.) at 1:1,000. FITC- or Texas red–conjugated goat anti–rabbit or goat anti–mouse IgG (Jackson ImmunoResearch Laboratories) was used as the secondary antibody. All images were collected with a Bio-Rad Laboratories MRC-1000 confocal imaging system.

Sciatic nerve ligation experiments

Sciatic nerve ligation experiments were done as previously described (Hanlon et al., 1997). In brief, one sciatic nerve from each animal was ligated; the other nerve was unligated and served as a control. After 6 h, ~0.5 cm of nerve segment was dissected from both sides (proximal and distal) near the ligature from each animal; two similar size segments were dissected from the control nerve in the comparable region. Nerve segments from each individual animal were homogenized in NP-40 lysis buffer (50 mM Tris-HCl, pH 8.0, 150 mM NaCl, 1% NP-40) and examined by Western blot analysis.

We thank members of the Goldstein and Cleveland labs for helpful comments during the course of this work. We especially thank Joe Marszalek for his valuable scientific and technical discussions, Gad Shiff for being an excellent mouse photographer, and Jagesh Shah for his efforts on biochemical studies.

C.-H. Xia was supported by a National Institutes of Health (NIH) predoctoral training grant in pharmacology and an NIH predoctoral cancer training grant. This work was supported by NIH grant GM35252 to L.S.B. Goldstein. L.S.B. Goldstein is an investigator of the Howard Hughes Medical Institute.

Submitted: 8 January 2003
Revised: 24 February 2003
Accepted: 24 February 2003

References

Bloom, G.S., and S.A. Endow. 1995. Motor proteins 1: kinesins. *Protein Profile.* 2:1105–1171.

Bloom, G.S., M.C. Gagner, K.K. Pfister, and S.T. Brady. 1988. Native structure and physical properties of bovine brain kinesin and identification of the ATP-binding subunit polypeptide. *Biochemistry.* 27:3409–3416.

Brady, S.T. 1985. A novel brain ATPase with properties expected for the fast axonal transport motor. *Nature.* 317:73–75.

Elder, G.A., V.L. Friedrich, Jr., P. Bosco, C. Kang, A. Gourov, P.H. Tu, V.M. Lee, and R.A. Lazzarini. 1998a. Absence of the mid-sized neurofilament subunit decreases axonal calibers, levels of light neurofilament (NF-L), and neurofilament content. *J. Cell Biol.* 141:727–739.

Elder, G.A., V.L. Friedrich, Jr., C. Kang, P. Bosco, A. Gourov, P.H. Tu, B. Zhang, V.M. Lee, and R.A. Lazzarini. 1998b. Requirement of heavy neurofilament subunit in the development of axons with large calibers. *J. Cell Biol.* 143: 195–205.

Eyer, J., and A. Peterson. 1994. Neurofilament-deficient axons and perikaryal aggregates in viable transgenic mice expressing a neurofilament-β-galactosidase fusion protein. *Neuron.* 12:389–405.

Fernyhough, P., A. Gallagher, S.A. Averill, J.V. Priestley, L. Hounsom, J. Patel, and D.R. Tomlinson. 1999. Aberrant neurofilament phosphorylation in sensory neurons of rats with diabetic neuropathy. *Diabetes.* 48:881–889.

Galbraith, J.A., T.S. Reese, M.L. Schlief, and P.E. Gallant. 1999. Slow transport of unpolymerized tubulin and polymerized neurofilament in the squid giant axon. *Proc. Natl. Acad. Sci. USA.* 96:11589–11594.

Goldstein, L.S.B., and A.V. Philp. 1999. The road less traveled: emerging principles of kinesin motor utilization. *Annu. Rev. Cell Dev. Biol.* 15:141–183.

Guo, L., L. Degenstein, J. Dowling, Q.C. Yu, R. Wollmann, B. Perman, and E. Fuchs. 1995. Gene targeting of BPAG1: abnormalities in mechanical strength and cell migration in stratified epithelia and neurologic degeneration. *Cell.* 81:233–243.

Hanlon, D.W., Z. Yang, and L.S.B. Goldstein. 1997. Characterization of KIFC2, a neuronal kinesin superfamily member in mouse. *Neuron.* 18:439–451.

Hoesche, C., A. Sauerwald, R.W. Veh, B. Krippl, and M.W. Kilimann. 1993. The 5′-flanking region of the rat synapsin I gene directs neuron-specific and developmentally regulated reporter gene expression in transgenic mice. *J. Biol. Chem.* 268:26494–26502.

Jacomy, H., Q. Zhu, S. Couillard-Després, J.M. Beaulieu, and J.P. Julien. 1999. Disruption of type IV intermediate filament network in mice lacking the neurofilament medium and heavy subunits. *J. Neurochem.* 73:972–984.

Julien, J.P. 1999. Neurofilament functions in health and disease. *Curr. Opin. Neurobiol.* 9:554–560.

Julien, J.P., and W.E. Mushynski. 1998. Neurofilaments in health and disease. *Prog. Nucleic Acid Res. Mol. Biol.* 61:1–23.

Kamal, A., G.B. Stokin, Z. Yang, C.H. Xia, and L.S.B. Goldstein. 2000. Axonal transport of amyloid precursor protein is mediated by direct binding to the kinesin light chain subunit of kinesin-I. *Neuron.* 28:449–459.

Kanai, Y., Y. Okada, Y. Tanaka, A. Harada, S. Terada, and N. Hirokawa. 2000. KIF5C, a novel neuronal kinesin enriched in motor neurons. *J. Neurosci.* 20: 6374–6384.

Koehnle, T.J., and A. Brown. 1999. Slow axonal transport of neurofilement protein in cultured neurons. *J. Cell Biol.* 144:447–458.

Lasek, R.J., P. Paggi, and M.J. Katz. 1992. Slow axonal transport mechanisms move neurofilaments relentlessly in mouse optic axons. *J. Cell Biol.* 117: 607–616.

Lasek, R.J., P. Paggi, and M.J. Katz. 1993. The maximum rate of neurofilament transport in axons: a view of molecular transport mechanisms continuously engaged. *Brain Res.* 616:58–64.

Meng, Y.X., G.W. Wilson, M.C. Avery, C.H. Varden, and R. Balczon. 1997. Suppression of the expression of a pancreatic β-cell form of the kinesin heavy chain by antisense oligonucleotides inhibits insulin secretion from primary cultures of mouse β-cells. *Endocrinology.* 138:1979–1987.

Navone, F., J. Niclas, N. Hom-Booher, L. Sparks, H.D. Bernstein, G. McCaffrey, and R.D. Vale. 1992. Cloning and expression of a human kinesin heavy chain gene: interaction of the COOH-terminal domain with cytoplasmic microtubules in transfected CV-1 cells. *J. Cell Biol.* 117:1263–1275.

Niclas, J., F. Navone, N. Hom-Booher, and R.D. Vale. 1994. Cloning and localization of a conventional kinesin motor expressed exclusively in neurons. *Neuron.* 12:1059–1072.

Nixon, R.A. 1992. Slow axonal transport. *Curr. Opin. Cell Biol.* 4:8–14.

Nixon, R.A. 1998a. The slow axonal transport of cytoskeletal proteins. *Curr. Opin. Cell Biol.* 10:87–92.

Nixon, R.A. 1998b. Dynamic behavior and organization of cytoskeletal proteins in neurons: reconciling old and new findings. *Bioessays.* 20:798–807.

Ohara, O., Y. Gahara, T. Miyake, H. Teraoka, and T. Kitamura. 1993. Neurofilament deficiency in quail caused by nonsense mutation in neurofilament-L gene. *J. Cell Biol.* 121:387–395.

Prahlad, V., M. Yoon, R.D. Moir, R.D. Vale, and R.D. Goldman. 1998. Rapid movements of vimentin on microtubule tracks: kinesin-dependent assembly of intermediate filament networks. *J. Cell Biol.* 143:159–170.

Prahlad, V., B.T. Helfand, G.M. Langford, R.D. Vale, and R.D. Goldman. 2000. Fast transport of neurofilament protein along microtubules in squid axoplasm. *J. Cell Sci.* 113:3939–3946.

Rahman, A., A. Kamal, E.A. Roberts, and L.S.B. Goldstein. 1999. Defective kinesin heavy chain behavior in mouse kinesin light chain mutants. *J. Cell Biol.* 146:1277–1288.

Rao, M.V., M.K. Houseweart, T.L. Williamson, T.O. Crawford, J. Folmer, and D.W. Cleveland. 1998. Neurofilament-dependent radial growth of motor axons and axonal organization of neurofilaments do not require the neurofilament heavy subunit (NF-H) or its phosphorylation. *J. Cell Biol.* 143:171–181.

Reid, E., M. Kloos, A. Ashley-Koch, L. Hughes, S. Bevan, I.K. Svenson, F.L. Graham, P.C. Gaskell, A. Dearlove, M.A. Pericak-Vance, et al. 2002. A kinesin heavy chain (KIF5A) mutation in hereditary spastic paraplegia (SPG10). *Am. J. Hum. Genet.* 71:1189–1194.

Vale, R.D., T.S. Reese, and M.P. Sheetz. 1985. Identification of a novel force-generating protein, kinesin, involved in microtubule-based motility. *Cell.* 42: 39–50.

Wang, L., C.-L. Ho, D. Sun, R.K.H. Liem, and A. Brown. 2000. Rapid movement of axonal neurofilaments interrupted by prolonged pauses. *Nat. Cell Biol.* 2:137–141.

Wurst, W., and A.L. Joyner. 1993. Production of targeted embryonic stem cell clones. *In* Gene Targeting: A Practical Approach. A.L. Joyner, editor. Oxford University Press, New York. 32–61.

Xia, C., A. Rahman, Z. Yang, and L.S.B. Goldstein. 1998. Chromosomal localization reveals three kinesin heavy chain genes in mouse. *Genomics.* 52:209–213.

Yabe, J.T., A. Pimenta, and T.B. Shea. 1999. Kinesin-mediated transport of neurofilament protein oligomers in growing axons. *J. Cell Sci.* 112:3799–3814.

Yagihashi, S. 1997. Pathogenetic mechanisms of diabetic neuropathy: lessons from animal models. *J. Peripher. Nerv. Syst.* 2:113–132.

Yang, Y., J. Dowling, Q.C. Yu, P. Kouklis, D.W. Cleveland, and E. Fuchs. 1996. An essential cytoskeletal linker protein connecting actin microfilaments to intermediate filaments. *Cell.* 86:655–665.

Yang, Y., C. Bauer, G. Strasser, R. Wollman, J.P. Julien, and E. Fuchs. 1999. Integrators of the cytoskeleton that stabilize microtubules. *Cell.* 98:229–238.

Zhu, Q., S. Couillard-Després, and J.P. Julien. 1997. Delayed maturation of regenerating myelinated axons in mice lacking neurofilaments. *Exp. Neurol.* 148:299–316.

Zhu, Q., M. Lindenbaum, F. Levavasseur, H. Jacomy, and J.P. Julien. 1998. Disruption of the NF-H gene increases axonal microtubule content and velocity of neurofilament transport: relief of axonopathy resulting from the toxin β,β'-iminodipropionitrile. *J. Cell Biol.* 143:183–193.

Zhu, Y., M.I. Romero, P. Ghosh, Z. Ye, P. Charnay, E.J. Rushing, J.D. Marth, and L.F. Parada. 2001. Ablation of NF1 function in neurons induces abnormal development of cerebral cortex and reactive gliosis in the brain. *Genes Dev.* 15:859–876.

Zochodne, D.W. 1996. Is early diabetic neuropathy a disorder of the dorsal root ganglion? A hypothesis and critique of some current ideas on the etiology of diabetic neuropathy. *J. Peripher. Nerv. Syst.* 1:119–130.